Hyperspectral Images Denoising via Global Tensor Ring Decomposition and Local Unsupervised Deep Image Prior

Jian-Li Wang[1], Ting-Zhu Huang[1], Xi-Le Zhao[1], Teng-Yu Ji[2], Tai-Xiang Jiang[3]

[1]School of Mathematical Sciences,
University of Electronic Science and Technology of China

[2]School of Mathematical Sciences,
Northwestern Polytechnical University

[3]School of Economic Information Engineering,
Southwestern University of Finance and Economics

Outline

- Background of HISs Denoising
- The Proposed Model and Algorithm
- Numerical Experiments

Background of HIS Denoising

- **Hyperspectral Images (HSIs)**
  - HSIs have widely used across many disciplines due to their advantages in providing rich spectral information, which is useful for distinguishing the substances in the scene.

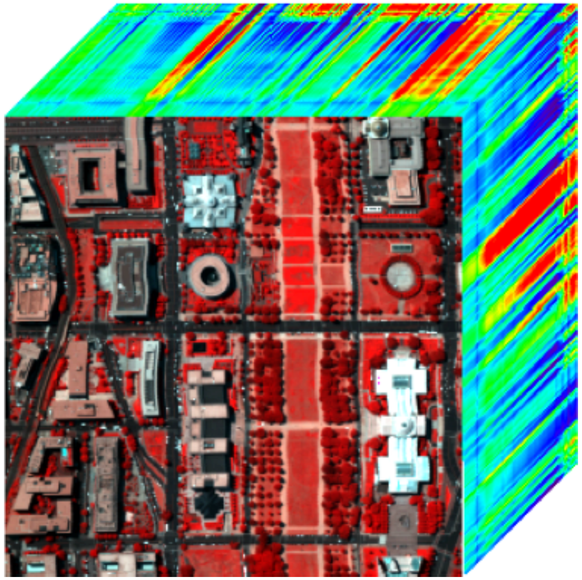

Background of HIS Denoising

- **Why Study HSI Denoising ?**
  - HSIs in real applications are unavoidably corrupted by various noises, i.e., Gaussian noise, salt and pepper noise, stripes, deadlines, and so on.

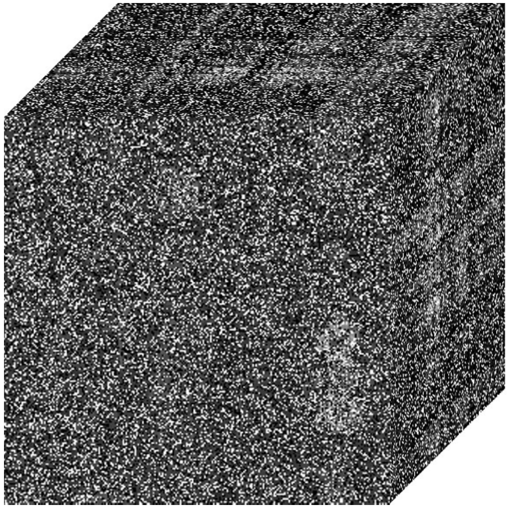

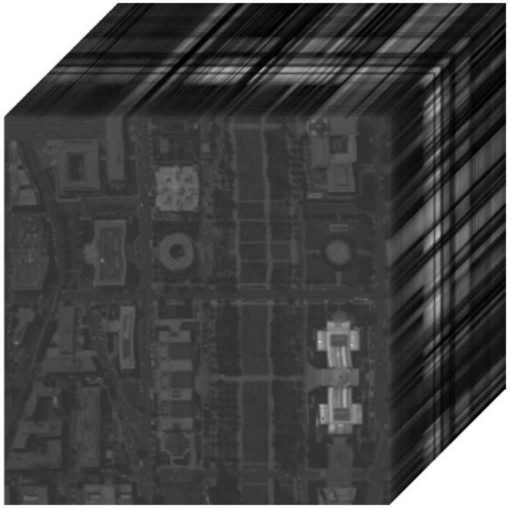

Background of HIS Denoising

- **Existing Works**
  - The traditional model-driven methods:
    - Require hand-crafted priors;
    - Relatively long running time;

Background of HIS Denoising

- **Existing Works**
  - The traditional model-driven methods:
    - Require hand-crafted priors;
    - Relatively long running time;
  - The deep learning (DL)-based methods:
    - Require many training samples;
    - May not have potentially mathematical interpretations.

Background of HIS Denoising

- **Deep Image Prior Framework**
  - Unsupervised DL method
  - Direct optimization loss function:

$$\boldsymbol{\theta}^* = \arg\min_{\boldsymbol{\theta}} \left\| \mathcal{F}_{\boldsymbol{\theta}}\left(\mathcal{Z}\right) - \mathcal{Y} \right\|_F^2$$

Background of HIS Denoising

- **Deep Image Prior Framework**
  - Unsupervised DL method
  - Direct optimization loss function:

$$\boldsymbol{\theta}^* = \arg\min_{\boldsymbol{\theta}} \|\mathcal{F}_{\boldsymbol{\theta}}(\mathcal{Z}) - \mathcal{Y}\|_F^2$$

- $\mathcal{Z}$ is a random input tensor;
- $\mathcal{Y}$ is the observed HSI;
- $\mathcal{F}$ is the CNN (i.e., U-Nets);

Background of HIS Denoising

- **Motivation**

3*3 2D Convolution

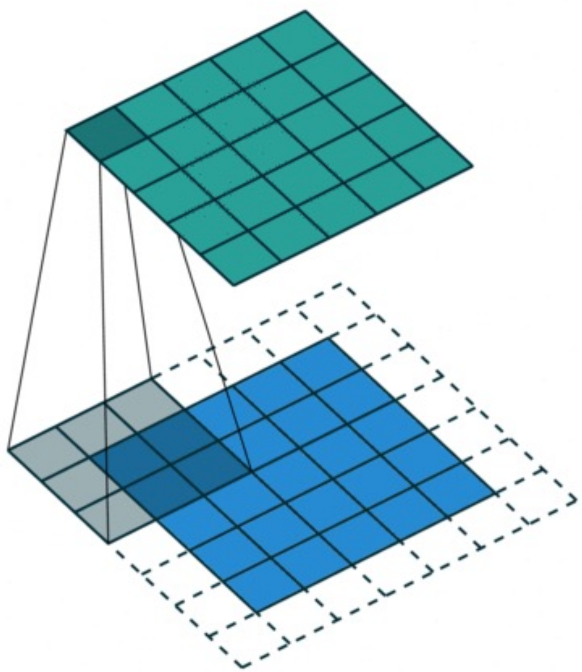

Dilated Convolution (L=2)

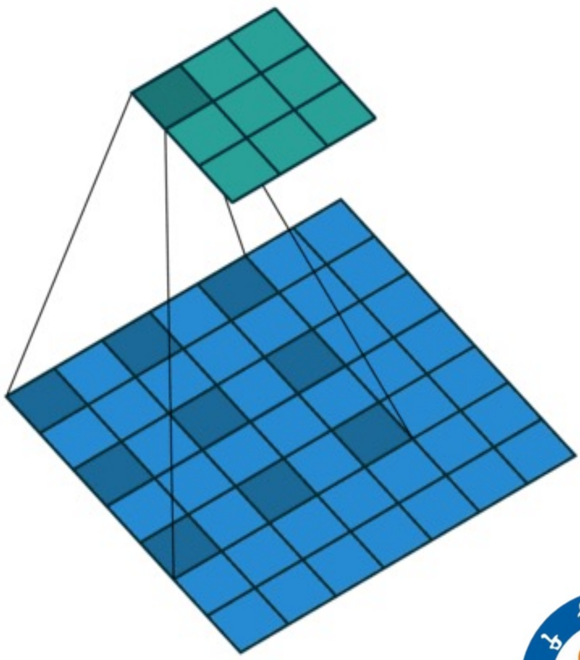

- **Proposed DIP-TR Model**

$$\underset{\mathcal{G},\mathcal{S},\boldsymbol{\theta}}{\operatorname{argmin}} \frac{1}{2}\|\mathcal{Y} - \mathcal{F}_{\boldsymbol{\theta}}(\mathcal{Z}) - \mathcal{S}\|_F^2 + \lambda\|\mathcal{F}_{\boldsymbol{\theta}}(\mathcal{Z}) - \Phi([\mathcal{G}])\|_F^2 + \mu\|\mathcal{S}\|_1,$$

The Proposed Model and Algorithm

- **Proposed DIP-TR Model**

$$\underset{\mathcal{G},\mathcal{S},\boldsymbol{\theta}}{\operatorname{argmin}} \frac{1}{2}\|\mathcal{Y} - \mathcal{F}_{\boldsymbol{\theta}}(\mathcal{Z}) - \mathcal{S}\|_F^2 + \lambda\|\mathcal{F}_{\boldsymbol{\theta}}(\mathcal{Z}) - \Phi([\mathcal{G}])\|_F^2 + \mu\|\mathcal{S}\|_1,$$

  - $\mathcal{Z}$ is a random input tensor generated by the network;
  - $\mathcal{G} := \{\mathcal{G}^{(1)}, \mathcal{G}^{(2)}, \mathcal{G}^{(3)}\}$ is core tensor of TR decomposition;
  - λ and μ are tuning parameters;
  - $\mathcal{F}_{\boldsymbol{\theta}}$ is a fixed CNN with parameter $\boldsymbol{\theta}$.

The Proposed Model and Algorithm

- **PAM-based Algorithm**
  - We develop an efficient PAM-based algorithm to resolve the proposed DIP-TR by alternately updating $\mathcal{G}, \mathcal{S}, \boldsymbol{\theta}$ as follows:

$$\mathcal{G}^{k+1} = \arg\min_{\mathcal{G}} \; \mathcal{L}(\mathcal{G}, \mathcal{S}^k, \boldsymbol{\theta}^k) + \frac{\rho}{2} \left\| \mathcal{G} - \mathcal{G}^k \right\|_F^2, \tag{4a}$$

$$\mathcal{S}^{k+1} = \arg\min_{\mathcal{S}} \; \mathcal{L}(\mathcal{G}^{k+1}, \mathcal{S}, \boldsymbol{\theta}^k) + \frac{\rho}{2} \left\| \mathcal{S} - \mathcal{S}^k \right\|_F^2, \tag{4b}$$

$$\begin{aligned} \boldsymbol{\theta}^{k+1} \in \arg\min_{\boldsymbol{\theta}} \; & \mathcal{L}(\mathcal{G}^{k+1}, \mathcal{S}^{k+1}, \boldsymbol{\theta}) \\ & + \frac{\rho}{2} \left\| \mathcal{F}_{\boldsymbol{\theta}}(\mathcal{Z}) - \mathcal{F}_{\boldsymbol{\theta}^k}(\mathcal{Z}) \right\|_F^2, \end{aligned} \tag{4c}$$

  - $\mathcal{L}(\mathcal{G}, \mathcal{S}, \boldsymbol{\theta})$ is the objective function;
  - ρ is the proximal parameter;
  - k is the iteration number.

The Proposed Model and Algorithm

- **PAM-based Algorithm**

Algorithm 1 The proposed DIP-TR denosing model based on the PAM optimization algorithm.

Input: The observed HSI $\mathcal{Y} \in \mathbb{R}^{M \times N \times B}$, TR rank $r = [r_1, r_2, r_3]$, the parameters λ, μ and ρ.

Initialization: $k = 0$, $\mathcal{F}_{\boldsymbol{\theta}^0}(\mathcal{Z}) = \mathcal{Y}$, $\mathcal{S}^0 = 0$, $(\mathcal{G}^{(1)})^0 = 0$, $(\mathcal{G}^{(2)})^0 = 0$, $(\mathcal{G}^{(3)})^0 = 0$, $k_{\max} = 100$, and $\varepsilon = 10^{-3}$.

while $\|\mathcal{F}_{\boldsymbol{\theta}^{k+1}}(\mathcal{Z}) - \mathcal{F}_{\boldsymbol{\theta}^k}(\mathcal{Z})\|_F / \|\mathcal{F}_{\boldsymbol{\theta}^k}(\mathcal{Z})\|_F > \varepsilon$ and $k \leqslant k_{\max}$ **do**

Update $\left(\mathcal{G}^{(n)}\right)^{k+1} = \mathrm{fold}_2\left(\left(2\lambda \mathcal{F}_{\boldsymbol{\theta}^k}(\mathcal{Z})_{<n>}\left(\mathbf{G}^{(\neq n)}_{<2>}\right)^k + \rho\left(\mathbf{G}^{(n)}_{(2)}\right)^k\right) \times \left(2\lambda\left(\mathbf{G}^{(\neq n)}_{<2>}\right)^{k,\top}\left(\mathbf{G}^{(\neq n)}_{<2>}\right)^k + \rho\mathbf{I}\right)^{-1}\right)$, $n = 1, 2, 3$,

where $\mathcal{G}^{(\neq n)}$ is obtained by multi-linear product of all core tensors except the n-th tensor in the order of $n+1$ to $n-1$.

Update $\mathcal{S}^{k+1} = \mathbf{shrink}\left(\frac{\mathcal{Y} - \mathcal{F}_{\boldsymbol{\theta}^k}(\mathcal{Z}) + \rho\mathcal{S}^k}{1+\rho}, \frac{\mu}{1+\rho}\right)$, where $[\mathbf{shrink}(\mathcal{X}, \xi)]_{i,j,m} = \mathbf{sign}(x_{i,j,m})\,\mathbf{max}(|x_{i,j,m}| - \xi, 0)$.

Update $\boldsymbol{\theta}^{k+1} \in \arg\min_{\boldsymbol{\theta}} \frac{1}{2}\|\mathcal{Y} - \mathcal{F}_{\boldsymbol{\theta}}(\mathcal{Z}) - \mathcal{S}^{k+1}\|_F^2 + \lambda\|\mathcal{F}_{\boldsymbol{\theta}}(\mathcal{Z}) - \Phi([\mathcal{G}^{k+1}])\|_F^2 + \frac{\rho}{2}\|\mathcal{F}_{\boldsymbol{\theta}}(\mathcal{Z}) - \mathcal{F}_{\boldsymbol{\theta}^k}(\mathcal{Z})\|_F^2$.

end while

Output: The restored HSI $\mathcal{F}_{\boldsymbol{\theta}}(\mathcal{Z})$.

Numerical Experiments

- **Compared Methods**

  - LRMR [Zhang et al. IEEE TGRS 2014];
  - LRTDTV [Wang et al. IEEE JSTARS 2018];
  - DIP-3D [Sidorov et al. IEEE ICCV 2019];
  - DIP-2D [Ulyanov et al. IEEE CVPR 2019].

Numerical Experiments

- **Dataset**
  - Indian Pines (145×145×224) and Washington DC Mall (256×256×191) as simulation data;
  - HYDICE Urban (307×307×210) as real data;

Numerical Experiments

- **Dataset**
  - Indian Pines (145×145×224) and Washington DC Mall (256×256×191) as simulation data;
  - HYDICE Urban (307×307×210) as real data;
- **Noise Case**
  - **Case 1**: Gaussian noise;
  - **Case 2**: Case 1+ the salt and pepper noise;
  - **Case 3**: Case2 + stripes and deadlines.

Numerical Experiments

Table 1. The PSNR (dB), SSIM, and SAM values of the recovered results for different noise settings by different methods.

Dataset	*Indain Pines*									*Washington DC Mall*								
Case	Case 1			Case 2			Case 3			Case 1			Case 2			Case 3		
Method	PSNR	SSIM	SAM	PSNR	SSIM	SAM	PSNR	SSIM	SAM	PSNR	SSIM	SAM	PSNR	SSIM	SAM	PSNR	SSIM	SAM
Observed	16.671	0.2707	16.9289	10.332	0.1099	31.6523	11.298	0.1353	29.1382	16.786	0.2704	40.5074	10.194	0.0876	51.2519	11.106	0.1083	50.3293
LRMR	33.615	0.8917	1.9383	31.013	0.8297	2.6645	28.602	0.8235	5.3366	32.978	0.9137	7.2692	30.755	0.8788	8.7605	30.074	0.8731	10.1731
LRTDTV	38.297	**0.9764**	1.2250	34.224	0.9243	2.3803	31.842	0.9081	4.2470	34.802	0.9326	5.9491	32.469	0.8936	8.9898	32.253	0.8844	12.2201
DIP-2D	33.652	0.9039	1.9670	23.984	0.7304	6.7097	23.056	0.7154	8.3755	33.947	0.9336	4.9650	22.473	0.7323	12.6629	24.138	0.7774	11.5496
DIP-3D	30.867	0.8982	2.6423	23.382	0.7354	6.8498	23.212	0.7264	6.5718	*	*	*	*	*	*	*	*	*
DIP-TR	**38.977**	0.9674	**1.0701**	**34.610**	**0.9609**	**1.7935**	**33.1176**	**0.9317**	**2.9616**	**35.8488**	**0.9526**	**4.0356**	**33.8411**	**0.9346**	**4.9402**	**32.8579**	**0.9264**	**6.2560**

Numerical Experiments

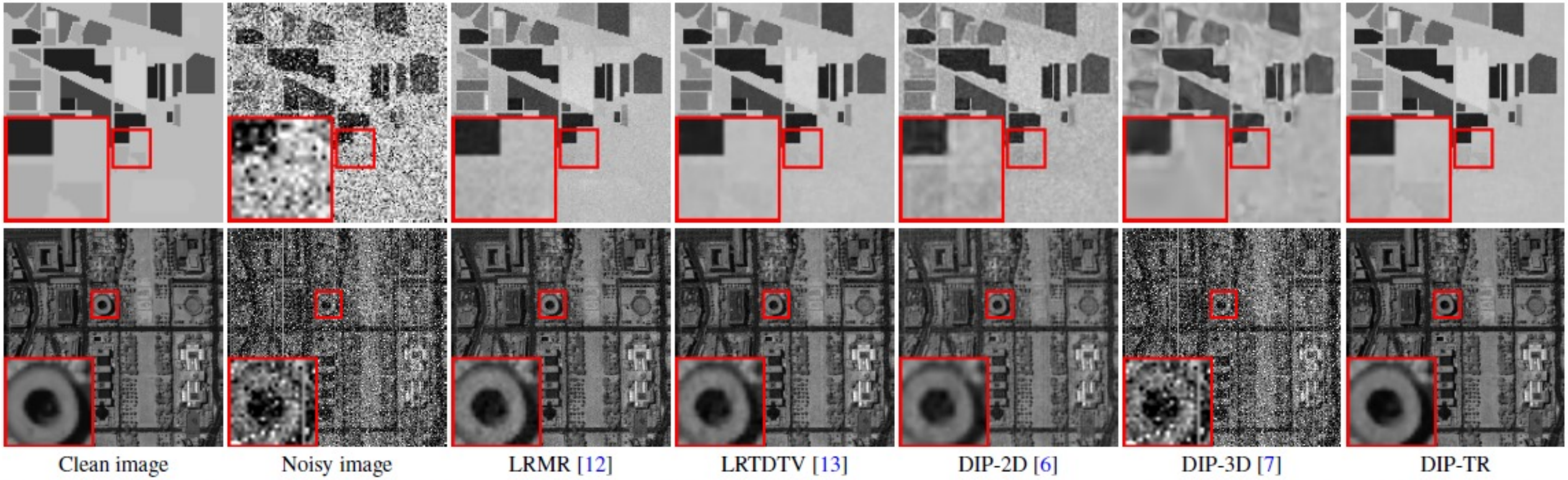

Fig. 2. The denoising results by different methods in the simulated experiments. Top row: band 57 in *Indain Pines* with Case 2. Bottom row: band 66 in *Washington DC Mall* with Case 3.

Numerical Experiments

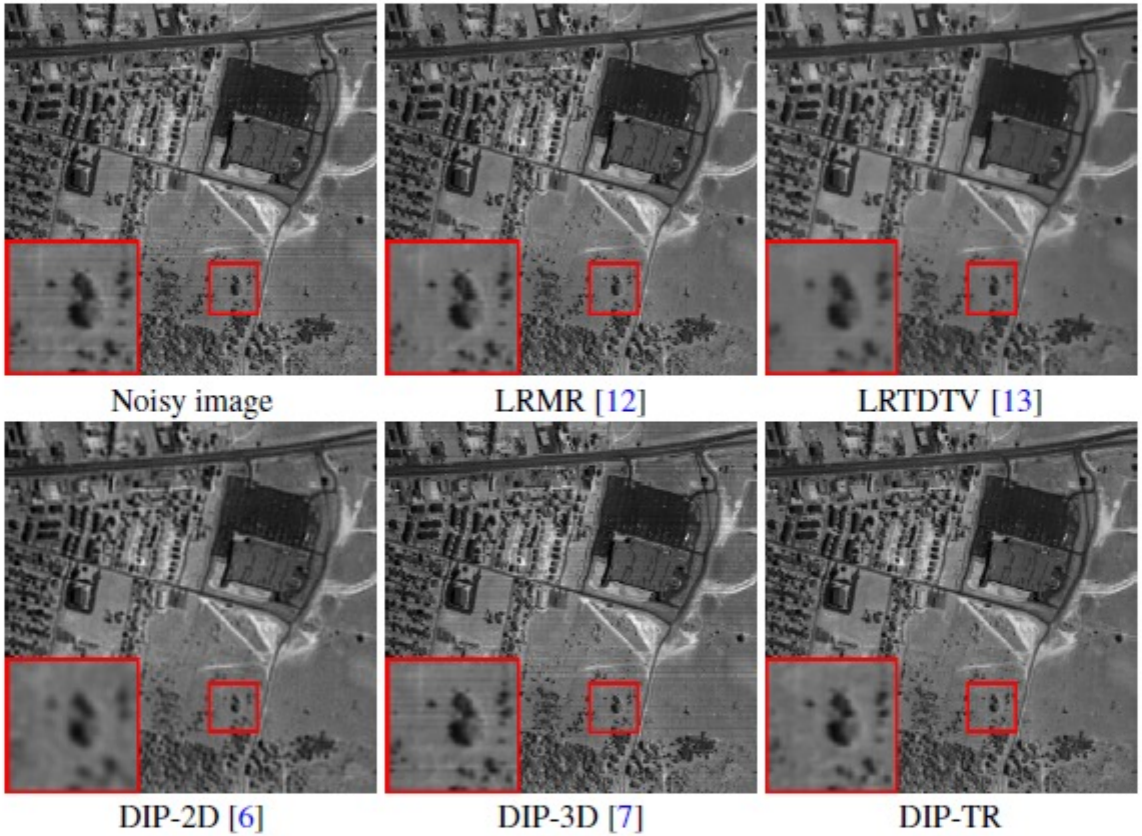

Fig. 3. The denoising results by different methods for band 103 of the real HSI *Urban*.

Thank you very much for listening

https://wangjianli123.github.io/homepage/